ChemPubSoc Europe

DOI: 10.1002/chem.201903458

CHEMISTRY A European Journal Full Paper

Fluorescent Probes

Highly Efficient Multiple-Labeling Probes for the Visualization of Enzyme Activities

Heng Song, Yuyao Li, Yefeng Chen, Chenghong Xue, and Hexin Xie*[a]

Abstract: Quinone methide (QM) as a latent trapping unit has been widely explored in activity-based self-immobilizing reagents. However, further application of this strategy has been largely hampered by the limited labeling efficiency to proteins. In this study, a thorough investigation on the labeling efficiency and the structure of QM-based trapping unit is presented, from which a QM with multiple leaving groups was identified as an optimal trapping unit. An alkaline phosphatase (ALP) immobilizing reagent featured with this multiple-labeling trapping unit exhibited lower nonspecific binding and, remarkably, a significantly higher labeling efficiency over other immobilizing reagents upon enzymatic activation. The utility of this imaging reagent was further demonstrated with the in vitro and in vivo visualization of the ALP activities. Furthermore, the multiple functional trapping unit may find greater value in the other activity-based immobilizing probes.

Introduction

Quinone methides (QMs),[1] including *ortho*-quinone methides (*o*-QMs) and *para*-quinone methides (*p*-QMs), are a class of highly reactive intermediates. These transient molecules have been widely utilized by nature. For instance, QMs have been employed as a means of defense by several animals and plants,[1b] and they are involved in the mechanism of action of the anticancer drug doxorubicin (Adriamycin), as well as of its derivative epirubicin.[2] Furthermore, QMs have been widely exploited in the efficient bioconjugation processes.[3]

The broad biological applications of QMs have been attributed to the exceptionally high electrophilicity of these molecules; these compounds have high potency in accepting nucleophiles from biological system. Taking advantage of this unique property, Danzin and co-workers reported in 1990 a class of *o*-QM-based enzyme-activatable inhibitors of β-glucosidases.[4] These inhibitors were specifically activated by β-glucosidase to liberate reactive *o*-QMs, which underwent nucleophilic addition by nucleophiles from active side of target enzyme to form covalent bonds and, thus, inhibited enzymatic activities. This mechanism-based approach was further applied in the development of potential inhibitors of phosphatase[5] and sulfatase.[6] Similar design has been exploited to capture catalytic antibodies[7] or enzymes in complex environment (e.g., live cells and tissues). However, this strategy was largely limited by the low specificity of QMs. This is likely due to the fact that these highly reactive intermediates form after diffusion out of the active site of target protein—unless they have specific affinity to the active site—and thus react with nucleophiles from nearby proteins.[8]

Nevertheless, this could be an advantage for imaging reagents; it may reflect the activities of enzyme more accurately without disturbing the structure of target enzyme. Along this line, QM has been extensively applied as self-immobilizing imaging reagents for activities of a number of biologically important enzymes, including phosphatases,[9] glycosidases,[8,10] sulfatases,[11] and β-lactamases.[12]

In general, these QM-based labeling probes structurally consist of four components: enzymatic recognition moiety, latent trapping moiety, linker, and reporter (Figure 1). The latent trapping moiety, that is, the precursor of QM, plays a key role in the efficiency of labeling covalently proteins. Currently, two types of QMs, *o*-QMs and *p*-QMs, are mainly employed as trapping units. The first type are usually *o*-monofluoromethylphenol or *o*-difluoromethylphenol derivatives; the activation by specific enzyme triggers the release of fluoride as the leaving group to form highly reactive *o*-QM in situ. The precursors of *p*-QM are usually caged 4-alkyl phenols with a leaving group, such as fluoro, carbamate, and carboxylic ester, on the benzyl position. With the potential leaving group far away from the enzymatic recognition moiety, the *p*-QM-derived latent trapping unit even allows for the installation of structurally hindered fluorescent quenchers on the leaving group, which leads to fluorogenic and self-immobilizing probe.[12a,13]

Over the past two decades, this QM-based labeling approach has been investigated in a wide variety of biological applications. In spite of this, a trapping molecule with higher labeling efficiency is still of high importance for further appli-

[a] H. Song, Y. Li, Y. Chen, C. Xue, Prof. Dr. H. Xie
State Key Laboratory of Bioreactor Engineering
Shanghai Key Laboratory of New Drug Design, School of Pharmacy
East China University of Science and Technology
Shanghai 200237 (P. R. China)
E-mail: xiehexin@ecust.edu.cn

Supporting information and the ORCID identification number(s) for the author(s) of this article can be found under: https://doi.org/10.1002/chem.201903458.

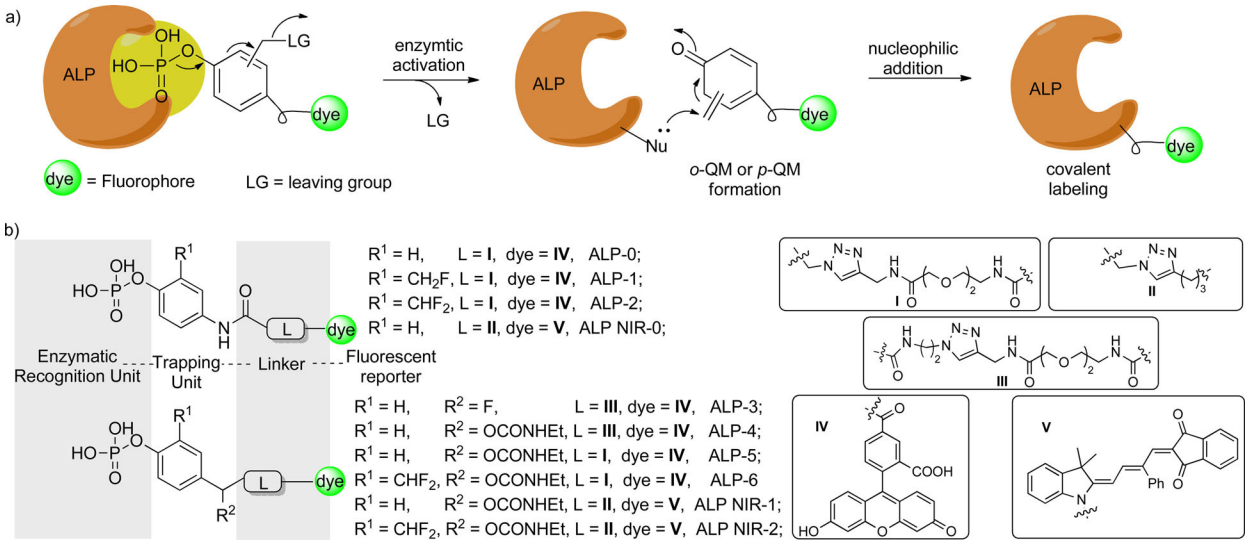

Figure 1. (a) Design of activity-based self-immobilizable probes for covalently labeling of alkaline phosphatase. (b) Chemical structures of self-immobilizing probes in this study.

cation of this strategy. However, to our surprise, systematic investigation of the labeling efficiency of QM-based immobilizing reagents, particularly in real biological environments, is rare. In this study, we have conducted a thorough investigation on the labeling efficiency of a range of QM-based trapping molecules, from which we have disclosed a QM precursor with multiple leaving groups that exhibits significantly higher labeling efficiency.

Alkaline phosphatase (ALP) is a type of hydrolase capable of dephosphorylation of a wide range of biological molecules, including nucleic acids and proteins, as well as other small molecules.[14] Current studies have indicated a number of diseases (e.g., osteoblastic bone cancer, prostatic cancer, and hepatitis) closely associate with increasing activities of ALP, and thus this enzyme can serve as an important biomarker for molecular biology and even clinical diagnosis.[15] To visualize activities of ALP, a number of assays have been developed, including fluorogenic probes,[16] self-assembly reagents,[16d,17] and QM-based self-immobilizing fluorescent probes.[9d,f] In this work, we employed ALP as a model enzyme for the investigation of labeling efficiency of QM-based trapping compounds.

Results and Discussion

Preparation of self-immobilizing probes

We prepared monofluoromethyl (ALP-1) and difluoromethyl (ALP-2) containing probes, as well as the *p*-QM-based probes (ALP-3 and ALP-4), according to reported procedures[9a,b,e] but with fluorescent reporter, fluorescein, connected by a Click reaction.[18] The leaving group-free probe (ALP-0) as the control reagent was also synthesized in a similar manner.

As outlined in Scheme 1, we started the synthesis of multiple-functional QM-bearing probe ALP-6 from nucleophilic substitution of **1**, followed by selective phosphorylation with diethyl phosphite in the presence of *N*,*N*-diisopropylethylamine (DIPEA) and 4-dimethylamino-pyridine (DMAP), to afford **2**. A Dess–Martin oxidation and subsequent fluorination with diethylaminosulfur trifluoride (DAST) furnished difluoromethyl-substituted **3**, which was further reduced by sodium borohydride to yield **4**. Treatment of **4** with ethyl isocyanate in the presence of triethylamine (TEA) gave fully functionalized **5**. Deprotection of **5** was achieved by bromotrimethylsilane and the resulting phosphate **6** was linked to an alkynyl-tethering fluorescein **7** by a simple Click reaction, as previously described. Probe ALP-6 was obtained after purification by reversed-phase HPLC and characterized by HRMS and HPLC analysis. Immobilizing probes ALP-5, ALP NIR-1, and ALP NIR-2, were synthesized and purified in a similar manner.

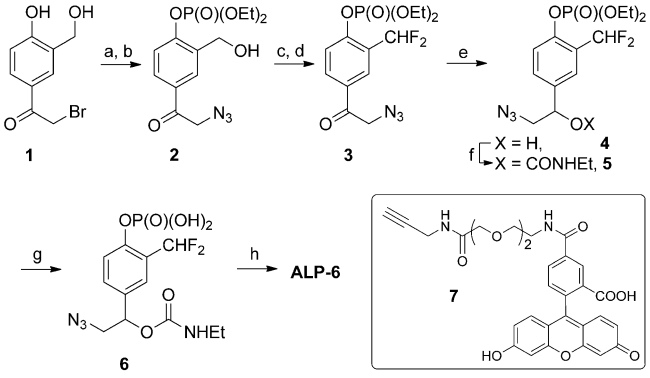

Scheme 1. Preparation of self-immobilizing probe ALP-6. a) NaN_3, DMF, RT; b) diethyl phosphite, DIPEA, DMAP, CCl_4/MeCN, −20 °C to RT; c) Dess–Martin periodinane (DMP), CH_2Cl_2, RT; d) diethylaminosulfur trifluoride (DAST), CH_2Cl_2, 0 °C; e) $NaBH_4$, MeOH, 0 °C; f) ethyl isocyanate, triethylamine (TEA), CH_2Cl_2, reflux; g) TMSBr, MeCN; h) **7**, $CuSO_4$, tris(3-hydroxypropyltriazolylmethyl)amine (THPTA), vitamin C, DMSO/H_2O (1:1), RT.

Evaluation of the labeling efficiency

To study the labeling efficiency of these self-immobilizing reagents, we incubated all of these probes (ALP-0, ALP-1, ALP-2, ALP-3, ALP-4, ALP-5, and ALP-6) with equal amount of ALP in phosphate buffered saline (PBS, pH 7.4) at 37 °C for 1 h and these samples were then subjected to sodium dodecyl sulfate–polyacrylamide gel electrophoresis (SDS-PAGE) analysis. It is worth noting that, to precisely represent the labeling of proteins in physiological environment, these samples were loaded on the SDS-PAGE gel without heating or incubation with reducing reagent (e.g., β-mercaptoethanol and dithiothreitol) to denature proteins. The labeling efficiency of these reagents was assessed by the in-gel fluorescence intensity. As shown in Figure 2a, the enzymes treated with *p*-QM-based probes (ALP-3, ALP-4, and ALP-5) emitted significantly stronger green fluorescence than the *o*-QM-based probes (ALP-1 and ALP-2)-incubated samples. As a control, the leaving group-free ALP-0 was totally ineffective on the introduction of fluorescence to ALP. As all of these immobilizing reagents only differ by the structure of latent trapping unit, these results seem to suggest the *p*-QM-based latent trapping moiety may be more efficient in labeling proteins than the *o*-QM-based counterparts, even though both have been widely used in biological studies.

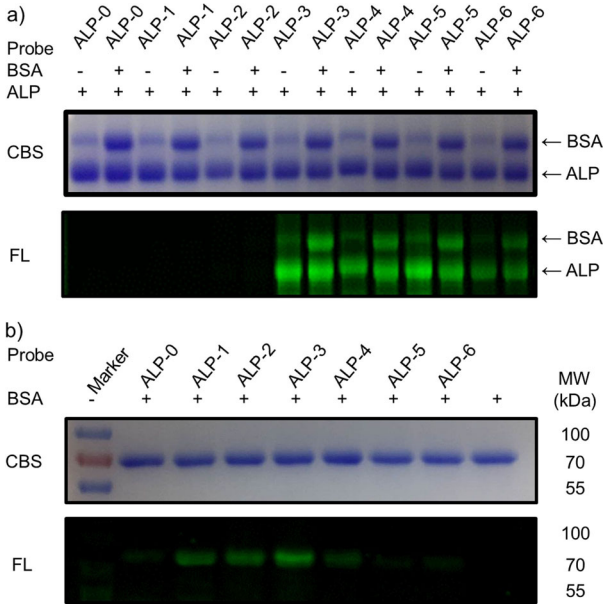

Figure 2. Labeling of proteins with immobilizing probes. (a) In-gel fluorescence scanning of ALP (12.5 U mL^{-1}) after incubation with indicated probes (7.5 μM) in the presence or absence of BSA (0.15 mg mL^{-1}) at 37 °C for 1 h. (b) In-gel fluorescence scanning of BSA (0.15 mg mL^{-1}) upon incubation with probes (7.5 μM) at 37 °C for 1 h. CBS: Coomassie blue staining; FL: fluorescence.

APL-6, unlike other trapping reagents, features leaving groups on both the *ortho*-position and the *para*-position, and thus may lead to the formation of *o*-QM and/or *p*-QM as trapping units upon enzymatic uncaging. We envisioned that this molecule may have multiple chances to generate highly reactive trapping unit upon one single enzymatic stimulus, providing multiple opportunities to label proteins and, thus, leading to improved labeling efficiency. However, to our surprise, on the basis of in-gel fluorescence imaging, the use of ALP-6 did not show any improvement on the labeling of ALP over other *p*-QM-based probes (ALP-3, ALP-4, and ALP-5).

Theoretically, these labeling reagents can be trapped by any available nucleophilic proteins after activation by ALP. To investigate the labeling of these molecules to other bystander proteins in the presence of ALP, we incubated all of these molecules with bovine serum albumin (BSA) along with ALP. The in-gel fluorescence image indicated that both proteins, BSA and ALP, were labeled by these ALP probes and the relative fluorescent intensity of these samples were similar to those incubated with ALP alone.

Labeling specificity is another important criteria for a covalently labeling reagent; poor specificity may lead to false information. To test their labeling specificity, we treated these labeling reagents with BSA without the addition of ALP, in which these reagents are not supposed to be activated to form *o*-QMs. The nonspecific labeling of these reagents to BSA was again assessed by in-gel fluorescence analysis (Figure 2b). There was hardly any fluorescence signal found in the ALP-0-treated BSA. However, the BSA-incubated with ALP-3 emitted stronger fluorescence than others, implying this *p*-QM-based labeling reagent may be less stable and thus led to non-specific bonding with BSA. Although the fluorescence on ALP-3-treated BSA was much weaker than those activated by ALP, it may still be problematic given to the high abundance of other bystander proteins in real samples. To our delight, molecule with the less reactive ethyl carbamate as the leaving group (ALP-4) generated less nonspecific fluorescence than the fluoro-containing counterpart (ALP-3). Notably, the replacement of the amido (L = III, ALP-4) with the triazole-bearing methylene group (L = I, ALP-5) as the linker further reduced nonspecific binding to BSA, leaving basically no fluorescence on the protein. With identical linker and leaving group as those in ALP-5, the multifunctional probe ALP-6 was also inert towards BSA. These results imply the non-specific binding of *p*-QM-based immobilizing reagents to BSA may associate with the electron properties of the linker, although other possibilities cannot be excluded at the current stage.

In addition to ALP, acid phosphatase (ACP) is also known as an efficient dephosphorylation enzyme. To investigate whether these reagents can be activated by ACP, and thus label ACP or other proteins, we incubated ALP-0 and ALP-6 with BSA in the presence of a catalytic amount of ACP in MES buffer (pH 5.0). In-gel fluorescence imaging (Figure S3, Supporting Information) indicated the sample incubated with ACP emitted significantly lower fluorescence than that with ALP in PBS (pH 7.4) though further analysis by HPLC revealed that the majority of ALP-6 has been consumed (Figure S2, Supporting Information). These results demonstrate the high labeling specificity of ALP-6 to ALP over ACP. We reason that the low labeling efficiency to ACP may be because the uncaged ALP-6 is stable in acidic conditions and cannot lead to the formation of reactive QM.

Considering the preliminary information on the labeling efficiency and specificity of these trapping reagents, we conduct-

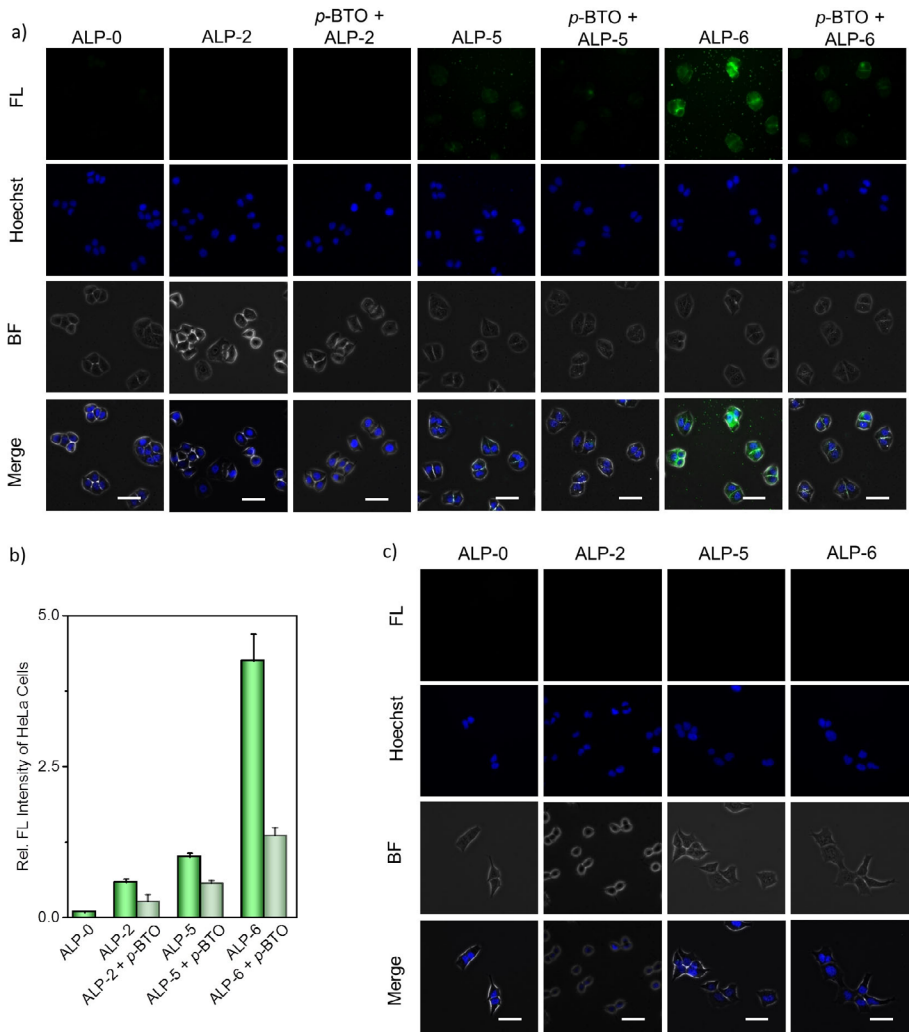

Figure 3. Fluorescent microscopic images of HeLa and HEK293 cells with immobilizable ALP probes. (a) Fluorescence images of HeLa cells incubated with indicated probes (10 μM) at 37 °C for 1.5 h, or pre-treated with ALP inhibitor *p*-BTO (500 μM) for 1 h before incubated with probes for 1.5 h. (b) Average fluorescence intensity of HeLa cells in (a). Error bars were calculated on *N* measurements, with *N* = 20, 16, 11, 16, 11, 12, and 12, from left to right. (c) Fluorescence images of HEK293 cells incubated with indicated probes (10 μM) at 37 °C for 1.5 h. FL: fluorescence; Hoechst: Hoechst 3342 staining; BF: bright field; *p*-BTO: (−)-*p*-bromotetramisole oxalate, an ALP inhibitor. Scale bar = 50 μm.

ed further investigations on their labeling of living cells. We incubated probes ALP-2, ALP-5, and ALP-6, as well as ALP-0 (as control), with ALP-overexpressing HeLa cells for 90 minutes. Upon washing away unbounded fluorescent reagents, all of these samples were then subjected to imaging with fluorescent microscope (Figure 3). As expected, the leaving group-free control probe (ALP-0) led to no retention of fluorescence on HeLa cells, whereas all of the other molecules introduced detectable green fluorescence on HeLa cells, but their intensity varied dramatically. The multiple-functional ALP-6 seemed to be the most efficient labeling reagent: the ALP-6-treated HeLa cells emitted about seven times stronger fluorescence than that with ALP-2 or over three times higher than ALP-5-incubated sample, whereas the labeling efficiency assessed by in-gel fluorescence imaging increased in the order: ALP-5 > ALP-6 ≫ ALP-2.

To further investigate the labeling specificity of these probes on cells, we pretreated HeLa cells with ALP inhibitor, (−)-*p*-bromotetramisole oxalate (*p*-BTO) before incubation with ALP-2, ALP-5, and ALP-6, which resulted in massively reducing of fluorescence on cells. Furthermore, ALP-negative HEK293 cells were also incubated with these labeling reagents, respectively, and none of these probes delivered noticeable fluorescence on HEK293 cells. These results demonstrate that the observed fluorescence signal on HeLa cells is indeed due to the dephosphorylation activities of ALP and further support the superior labeling ability of ALP-6.

ALP is known to overexpress on the extracellular membrane of HeLa cells,[17,19] the difference on the permeability of these labeling reagents—if there is any difference—is unlikely the reason for the variety of labeling efficiency on cells. To elucidate the inconsistent results obtained from live cell fluorescent imaging and in-gel fluorescence imaging, we further incubated lysate of HeLa cells with ALP-5 or ALP-6 and then analyzed the fluorescent labeling of proteins by in-gel fluorescence imaging. As illustrated in Figure S1 (Supporting Information), both imag-

ing reagents produced substantial amount of fluorescence on proteins. However, clearly ALP-5 led to stronger fluorescence than ALP-6, which is in agreement with aforementioned in-gel fluorescence analysis of ALP but different from the fluorescent imaging of living cells. These results imply that some of the fluorescence-labeled proteins on living cells may not be detectable from PAGE gel, presumably due to the low stability of these fluorescent complex. In other words, fluorescent microscope imaging of living cells is a more suitable approach than in-gel fluorescence analysis to evaluate the labeling ability of activity-based immobilizing reagents.

To rationalize the difference of fluorescent labeling to proteins, plausible mechanisms were proposed in Scheme 2.[1b,4]

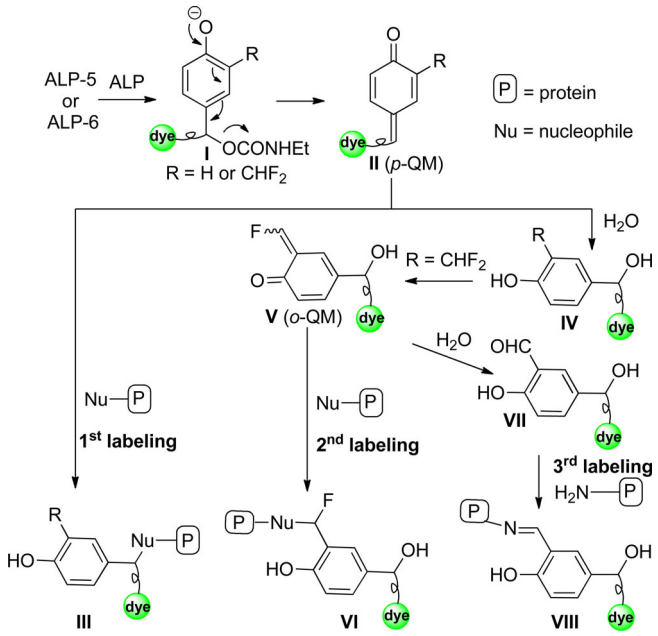

Scheme 2. Plausible fluorescent labeling mechanisms of ALP-5 and ALP-6.

Considering stability of the highly reactive intermediate, we tend to believe *p*-QM (**II-1** or **II-2**) may form first for both ALP-5 and ALP-6 upon activation by ALP. These *p*-QMs then undergoes nucleophilic addition by nucleophiles from nearby proteins (first labeling) before diffusion out and addition by abundant water to form compound **IV-1** or **IV-2**. The ALP-5-leading **IV-1** will eventually be washed away from cells. However, for the ALP-6-leading **IV-2**, it could form reactive QM (**V**) again and undergo nucleophilic addition by proteins (second labeling), though the chance may be slim as it is far away from proteins. Most of the QM (**V**) may be attacked by water again to give aldehyde (**VII**). This aldehyde is supposed to be inert to water but may react with amino group of proteins (three labeling). Having multiple chances to label proteins upon one single stimulus may be the origin of superior labeling ability of ALP-6. It is worth noting that the imine-based dye–protein complex may not be stable enough during gel electrophoresis. This may be the reason why ALP-6 exhibited stronger fluorescence on the cell-based imaging but had weaker fluorescence signal on in-gel imaging, though other possibilities cannot be ruled out completely at the current stage.

Near-infrared labeling reagents

Fluorescent dyes with absorption and emission at the range of near-infrared zone are particularly useful for biomedical investigations due to the high tissue-penetration ability and less interference by the intrinsic autofluorescence from living animals.[20] Therefore, to further expand the application of our design, we replaced the fluorescent reporter with near-infrared and switchable P-Mero4.[21]

We performed in-gel fluorescence analysis again to evaluate these near-infrared imaging reagents. As depicted in Figure 4a, both ALP NIR-1 and multiple-functional ALP NIR-2 showed excellent labeling ability to proteins, delivering strong near-infrared fluorescence on ALP or BSA. The specificity of the labeling was further confirmed by the use of ALP inhibitor (*p*-BTO) or the leaving-group-free control probe (ALP NIR-0).

P-Mero4 is a highly environment-sensitive fluorophore; its fluorescence can be dramatically enhanced after covalently interaction with proteins. To reveal the fluorescent response of the near-infrared self-immobilizing molecule, we recorded the fluorescent spectra of ALP NIR-2 in the absence or presence of ALP (Figure 4b). As expected, ALP NIR-2 in PBS (pH 7.4) alone was basically nonfluorescent and the addition of ALP boosted its fluorescence at 660 nm intensively. As a control, the incuba-

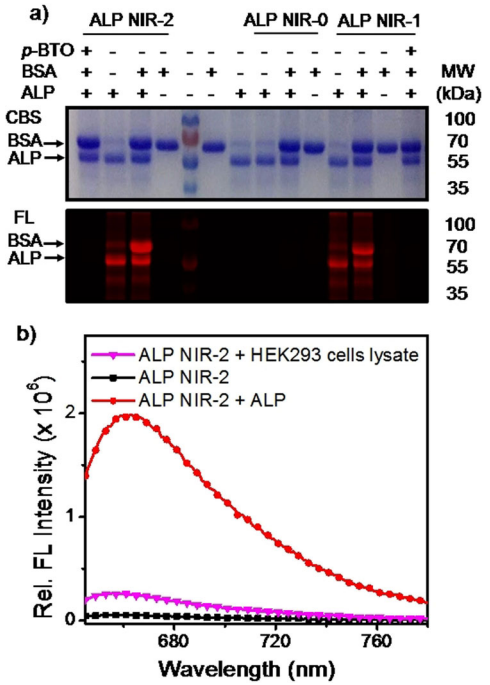

Figure 4. (a) In-gel fluorescence imaging of ALP upon incubation with immobilizing probes. Indicated proteins (BSA: 0.15 mg mL^{-1}; ALP 5 U mL^{-1}) were incubated with probes (5 μM) at 37 °C for 2 h, or proteins were pre-treated with *p*-BTO (5 mM) for 1 h before incubation with probes for 2 h. (b) Fluorescence spectra of ALP NIR-2 (1 μM) before or after incubation with ALP (50 μg, 2.5 U mL^{-1}) or HEK293 cells lysate (50 μg, 0.25 mg mL^{-1}) at 37 °C for 30 min (λ_{ex} = 635 nm). CBS: Coomassie blue staining; FL: fluorescence.

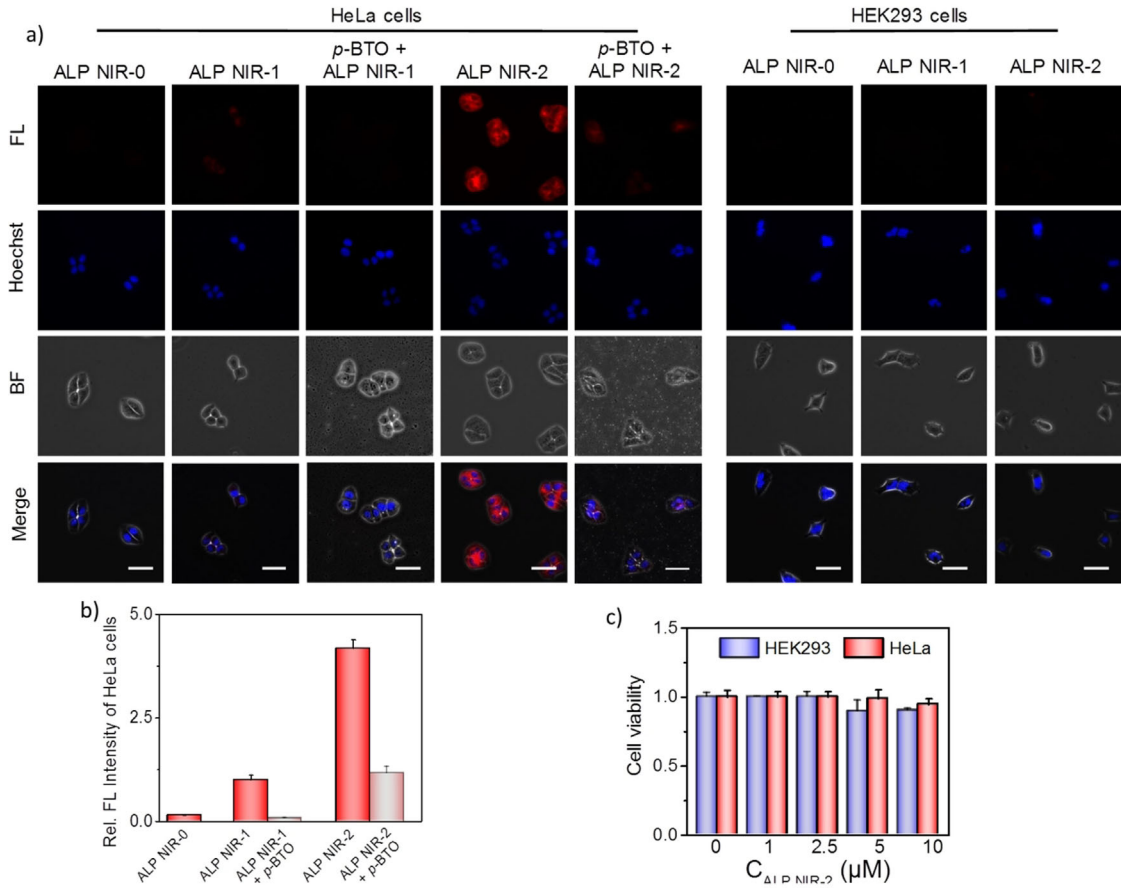

Figure 5. (a) Fluorescent microscope images of HeLa cells or HEK293 cells upon incubation with immobilizable ALP NIR probes. Indicated cells were incubated with trapping probes (5 μM) at 37 °C for 1.5 h, or pretreated with ALP inhibitor *p*-BTO (500 μM) for 1 h before incubation with probes for 1.5 h. (b) Average fluorescence intensity of HeLa cells in (a). Error bars were calculated on *N* measurements, with *N* = 6, 6, 9, 18, and 10, from left to right. (c) HEK 293 cell viability upon treatment with ALP NIR-2. HeLa cells or HEK293 cells were incubated with ALP NIR-2 at 0, 1, 2.5, 5, 10 μM for 24 h, and the cell viability was determined by MTT assay. FL: fluorescence; Hoechst: Hoechst 3342 staining; BF: bright field; scale bar = 50 μm; error bars were calculated on three experiments.

tion of ALP NIR-2 with lysate of HEK293 (ALP-negative cells) led to a considerably lower enhancement of fluorescence. However, given the large abundance of nonspecific proteins on cells, washing away unbounded fluorescent molecules may still be necessary for these NIR imaging reagents in cell imaging.

Following aforementioned protocol, the labeling ability and specificity of ALP NIR-1 and ALP NIR-2 were studied by the fluorescent imaging of living HeLa cells (Figure 5 a,b). Similar to ALP-6, ALP NIR-2 produced a much stronger fluorescent signal than the *p*-QM-based ALP NIR-1, confirming again the superior labeling ability of the multiple-functional trapping unit.

Moreover, the cytotoxicity of this trapping reagent was studied by incubation HeLa cells or HEK293 cells with a serial concentrations of ALP NIR-2 and it turned out that this compound has negligible cytotoxicity to both HEK293 cells and HeLa cells even at the concentration of 10 μM (Figure 5 c).

In vivo imaging of enzyme activities

The increasing activities of ALP is closely related to a range of tumors. However, in vivo tracking activities of ALP on tumor has been a challenge due to the fact that this enzyme usually overexpresses on the extracellular membrane of tumor cells:[16,17] fast diffusion likely occurs for most of the activatable imaging reagents. The QM-based self-immobilizing probes are capable to generate covalent linkage with ALP-overexpressing cells upon activation, which may provide an opportunity to visualize activities of ALP in living animals.

To examine the feasibility of the self-immobilizing probe in imaging of activities of endogenous ALP in vivo, BALB/c nude mice bearing HeLa tumor were intratumorally injected with ALP NIR-2 and ALP NIR-0 (as control), respectively. We monitored the fluorescence intensity of mice at 670 nm over the time course of 24 h after injection. As shown in Figure 6, though ALP NIR-0 and ALP NIR-2 were injected in identical amounts (30 mM, 100 mL), the ALP NIR-2-treated tumor emitted highly stronger fluorescence than that with leaving group-free ALP NIR-0 even at 10 minutes after the injection. This remarkably difference may result from the slower cleanup rate of ALP NIR-2, and more importantly, the enhancement of fluorescence intensity induced by the formation of covalent bond with proteins after enzymatic activation. The retention of fluorescence on the ALP NIR-2-treated tumor was much longer

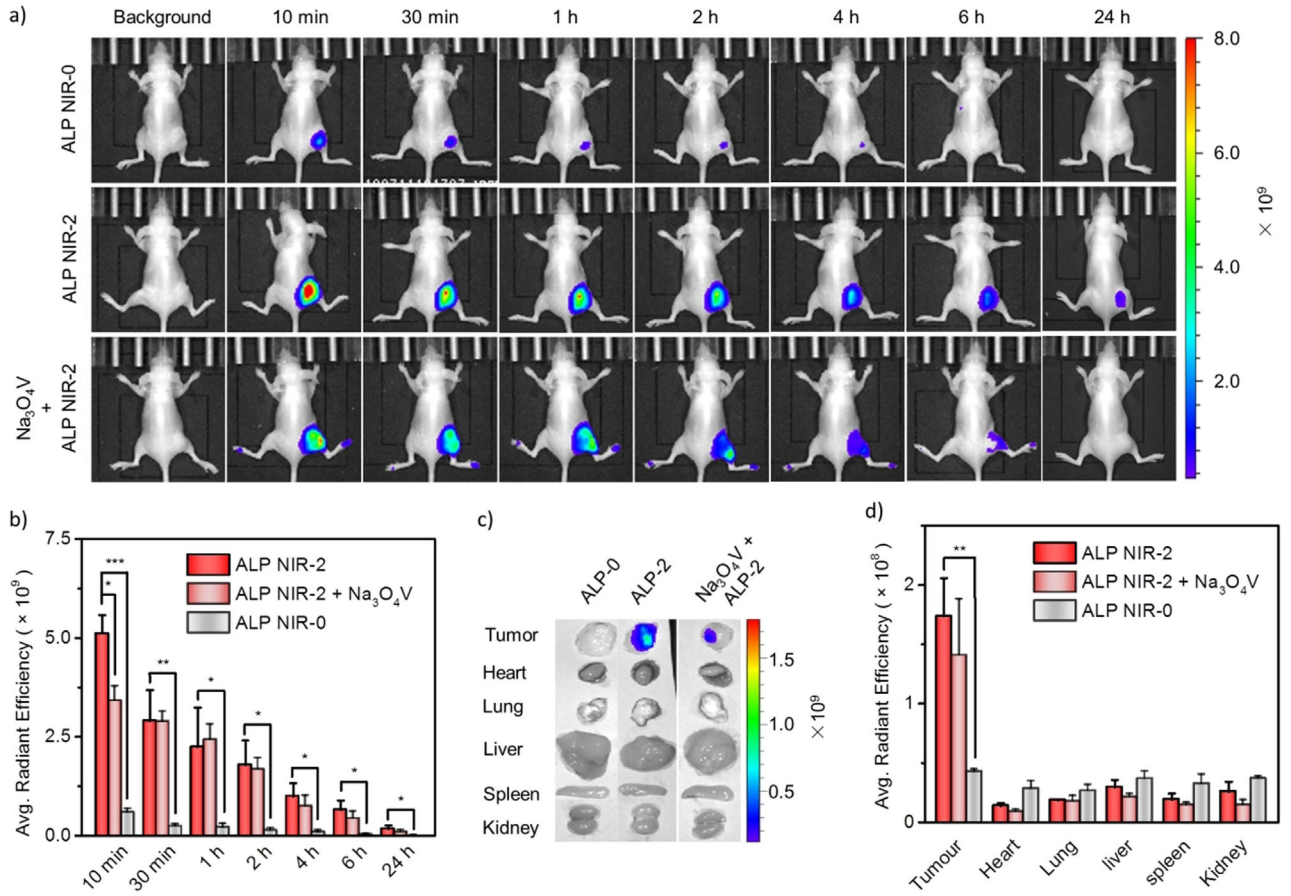

Figure 6. Fluorescence imaging of HeLa tumor xenograft mice upon injection of immobilizing probe ALP NIR-2. (a) Whole-body fluorescence imaging of HeLa tumor-bearing mice. (b) Average fluorescence intensity of HeLa tumors on mice. (c) Fluorescence imaging of main organs of mice 24 h after the injection of probes. (d) Average fluorescence intensity of main organs of mice at 24 h after the injection of probes. ALP NIR-0 or ALP NIR-2 (30 μM, 100 μL) was intratumorally injected or pre-treated tumor with ALP inhibitor Na_3O_4V (10 mM, 50 μL) for 10 min for injection of probes. $\lambda_{ex}=620$ nm, $\lambda_{em}=670$ nm; error bars were calculated on three experiments; $^*P<0.05$; $^{**}P<0.01$; $^{***}P<0.001$).

than that injected with ALP NIR-0; fluorescence signal can be detected even 24 h after injection. Furthermore, the intratumoral injection of an ALP inhibitor, sodium orthovanadate (Na_3O_4V), before that of ALP NIR-2, reduced the fluorescence of tumor at 10 minutes after the injection though the effect of this inhibitor diminished after half an hour, which is likely because this small molecule was cleared up from tumor rapidly.

Conclusions

In summary, we have conducted an unprecedented investigation on the structure of QM precursors and the labeling efficiency and specificity by using ALP as a model enzyme. Based on the in-gel fluorescence analysis and living cell fluorescent imaging, we have identified a new multiple functional QM as the optimal latent trapping unit. An ALP self-immobilizing reagent with such a trapping unit allows for the labeling of proteins in multiple ways upon enzymatic activation, and leads to lower nonspecific binding and, more importantly, significantly higher labeling efficiency on living cells than current *o*-QM or *p*-QM-based labeling reagents. Preliminary in vivo studies have demonstrated that this type of self-immobilizing reagent can be used to visualize the activities of ALP in living animals. Moreover, this multiple functional QM precursor may serve as a general trapping unit in the other activity-based immobilizing probes.

Experimental Section

Synthesis and characterization

2-Azido-1-{4-[(diethoxyphosphoryl)oxy]-3-(difluoromethyl)-phenyl}ethyl ethylcarbamate (5): To a solution of **3** (202 mg, 0.56 mmol) in methanol (5 mL) at 0 °C was added $NaBH_4$ (32 mg, 0.83 mmol) in several portions and the resulting mixture were stirred at the same temperature for 30 min. A saturated aqueous solution of NH_4Cl (2 mL) was then added. The organic layer was separated and the aqueous phase was extracted with DCM (10 mL × 3). The combined organic layers were dried over $MgSO_4$ and purified by chromatography on a short silica gel column to afford **4** as crude product, which was used in next step without further purification.

Under N_2 atmosphere, a solution of **4** (161 mg, 0.44 mmol), ethyl isocyanate (175 μL, 2.2 mmol) and TEA (307 μL, 2.2 mmol) in CH_2Cl_2 (anhydrous, 3 mL) were heated to reflux for 12 h. After cooling to

room temperature, water (2 mL) was then added dropwise. The organic layer was separated and the aqueous phase was extracted with CH_2Cl_2 (10 mL × 3). The combined organic layers were dried over $MgSO_4$ and purified by chromatography on silica gel column to give **5** (115 mg, 47% form **3**). ^{1}H NMR (400 MHz, $CDCl_3$) δ = 7.60 (s, 1H), 7.50–7.42 (m, 2H), 6.93 (t, J = 55.1 Hz, 1H), 5.88–5.83 (m, 1H), 4.87 (s, 1H), 4.28–4.18 (m, 4H), 3.61–3.43 (m, 2H), 3.30–3.18 (m, 2H), 1.36 (t, J = 7.1 Hz, 6H), 1.15 ppm (t, J = 7.2 Hz, 3H). ^{13}C NMR (100 MHz, $CDCl_3$) δ = 154.82, 148.54 (q, J = 5.9 Hz), 135.07, 130.22, 125.64 (td, J = 22.9, 7.2 Hz), 124.66 (t, J = 5.8 Hz), 120.41 (d, J = 1.8 Hz), 111.06 (t, J = 237.7 Hz), 73.86, 65.11 (d, J = 6.2 Hz), 55.21, 36.00, 16.00 (d, J = 6.6 Hz), 15.03 ppm. HRMS (ESI) *m/z* calcd for $C_{16}H_{23}F_2N_4O_6P$ $[M+Na]^+$: 459.1215, found 459.1223.

2-Azido-1-[3-(difluoromethyl)-4-(phosphonooxy)phenyl]ethyl ethylcarbamate (6): Under N_2 atmosphere, to a solution of **5** (115 mg, 0.26 mmol) in acetonitrile (anhydrous, 2 mL) at 0 °C was added TMSBr (174 μL, 1.3 mmol) and the resulting mixtures were stirred at room temperature for 12 h. A saturated aqueous solution NH_4Cl (2 mL) was then added, followed by CH_2Cl_2 (5 mL). The organic layer was separated and the aqueous phase was extracted with CH_2Cl_2 (10 mL×3). The title compound was obtained by RP-HPLC purification on a C18 column (34 mg, 35%). ^{1}H NMR (400 MHz, [D$_6$]DMSO) δ = 7.60 (s, 1H), 7.54 (d, J = 8.4 Hz, 1H), 7.48–7.39 (m, 2H), 7.11 (t, J = 55.1 Hz, 1H), 5.80 (t, J = 5.6 Hz, 1H), 3.64 (d, J = 5.6 Hz, 2H), 3.00 (qd, J = 10.8, 7.0 Hz, 2H), 1.00 ppm (t, J = 7.2 Hz, 3H). ^{13}C NMR (100 MHz, [D$_6$]DMSO) δ = 154.93, 149.29 (q, J = 6.0 Hz), 134.74, 130.24, 125.10 (td, J = 22.7, 6.2 Hz), 123.96 (t, J = 4.7 Hz), 120.97, 111.65 (t, J = 235.1 Hz), 72.79, 54.49, 35.25, 15.02 ppm. HRMS (ESI) *m/z* calcd for $C_{12}H_{15}F_2N_4O_6P$ $[M-H]^-$: 379.0625; found 379.0620.

5-{2-[2-(2-{[(1-{2-[3-(Difluoromethyl)-4-(phosphonooxy)phe-nyl]-2-[(ethylcarbamoyl)oxy]ethyl}-1*H*-1,2,3-triazol-4-yl)methyl]amino}-2-oxoethoxy)ethoxy]ethyl)carbamoyl}-2-(6-hydroxy-3-oxo-3*H*-xanthen-9-yl)benzoic acid (ALP-6): To a solution of **7** (1.5 mg, 2.76 μmol), L-(+)-ascorbic acid (vitamin C, 1.3 mg, 7.2 μmol), $CuSO_4$ (30 μg, 0.18 μmol), and tris(3-hydroxypropyltriazolyl methyl)amine (THPTA, 80 μg, 0.18 μmol) in 15 μL DMF were added **6** (0.68 mg in 5 μL DMF, 1.8 μmol) and water (15 μL). The resulting mixture was stirred at room temperature for 30 min. The title compound ALP-6 (1.0 mg, 40%) was obtained after RP-HPLC purification on a C18 column. HRMS (ESI) *m/z* calcd for $C_{42}H_{41}F_2N_6O_{15}P$ $[M-H]^-$ 937.2263; found 937.2256.

Fluorescence microscope imaging of live cells

Cells were incubated in DMEM, supplemented with 10% fetal bovine serum (FBS) and 1% penicillin-streptomycin (PS), at 37 °C with 5% CO_2 and passaged upon reaching 70–80% confluence. Immobilizing probes (10 μM for ALP-0, 2, 5, 6; 5 μM for ALP NIR-0, 1, 2) were incubated with cells at 37 °C for 1.5 h and then washed with PBS (pH 7.4) for 3 times before being subjected to fluorescence microscope imaging. For the experiments with inhibitor, cells were pre-treated with *p*-BTO (500 μM) at 37 °C for 1 h before incubation with probes.

In vitro cytotoxicity assay

The cytotoxicity of ALP NIR-2 to HEK293 cells or HeLa cells was assessed by 3-(4,5-dimethylthiazol-2-yl)-2,5-diphenyltetrazolium bromide (MTT) Cell Proliferation and Cytotoxicity assay. Following the manufacturer's protocol, cells (5×10^3 cells per well) in Dulbecco's modified Eagle's medium (DMEM; supplemented with 10% FBS, 100 μL) were plated in 96-well plates and incubated at 37 °C overnight. Media was then changed and cells were treated with ALP NIR-2 at a serial of concentrations (0, 1, 2.5, 5, and 10 μM) in DMEM (supplemented with 10% FBS, 100 μL). After incubation at 37 °C for 24 h, MTT (10 μL, 5 mg mL^{-1} in PBS) was added to each well and incubated at 37 °C for 4 h. The solution was then removed and DMSO (100 μL) was added to dissolve the resulting purple crystal. Absorbance at 490 nm was measured with a microplate reader to assess the cell viability. Each experiment was run in triplicate.

Real-time in vivo imaging of tumor-bearing mice

All animal experiments were performed in accordance with the guidelines of Care and Use of Laboratory Animals of China for animal experimentation and approved by the ethics committee of the East China University of Science and Technology Animal procedures.

BALB/c female mice bearing subcutaneous HeLa tumors (see Supporting Information for detail) were used in this study (n = 3 for each group). Immobilizing probes ALP NIR-0 or ALP NIR-2 was intratumorally injected (30 μM in PBS, 100 μL) and fluorescence imaging of whole mice was performed with IVIS Lumina XRMS Series III In Vivo Imaging System (PerkinElmer, Inc. USA) with excitation at 620 nm and emission at 670 nm at different time points (10 min, 30 min, 1 h, 2 h, 4 h, and 24 h). The inhibition experiments were conducted by intratumoral injection of ALP inhibitor Na_3O_4V (50 μL, 10 mM in Tris buffer, pH 8.0) for 10 min before injection of ALP NIR-2.

Acknowledgements

Financial support from The Recruitment Program for Young Professionals, NSFC-BRICS (81861148020), the Research Program of State Key Laboratory of Bioreactor Engineering, and the Fundamental Research Funds for the Central Universities are gratefully acknowledged.

Conflict of interest

The authors declare no conflict of interest.

Keywords: alkaline phosphatase · enzyme activity · imaging · immobilization · quinone methide

[1] a) *Quinone Methides* (Ed.: S. E. Rokita), Wiley, Hoboken, **2009**; b) R. W. Van de Water, T. R. R. Pettus, *Tetrahedron* **2002**, *58*, 5367–5405.
[2] D. J. Taatjes, G. Gaudiano, K. Resing, T. H. Koch, *J. Med. Chem.* **1996**, *39*, 4135–4138.
[3] a) Q. Li, T. Dong, X. Liu, X. Lei, *J. Am. Chem. Soc.* **2013**, *135*, 4996–4999; b) Q. Li, T. Dong, X. H. Liu, X. Y. Zhang, X. Y. Yang, X. G. Lei, *Curr. Org. Chem.* **2014**, *18*, 86–92; c) X. Zhang, T. Dong, Q. Li, X. Liu, L. Li, S. Chen, X. Lei, *ACS Chem. Biol.* **2015**, *10*, 1676–1683.
[4] S. Halazy, V. Berges, A. Ehrhard, C. Danzin, *Bioorg. Chem.* **1990**, *18*, 330–344.
[5] J. K. Myers, T. S. Widlanski, *Science* **1993**, *262*, 1451–1453.
[6] V. Ahmed, Y. Liu, S. D. Taylor, *ChemBioChem* **2009**, *10*, 1457–1461.
[7] K. D. Janda, L. C. Lo, C. H. L. Lo, M. M. Sim, R. Wang, C. H. Wong, R. A. Lerner, *Science* **1997**, *275*, 945–948.
[8] D. H. Kwan, H. M. Chen, K. Ratananikom, S. M. Hancock, Y. Watanabe, P. T. Kongsaeree, A. L. Samuels, S. G. Withers, *Angew. Chem. Int. Ed.* **2011**, *50*, 300–303; *Angew. Chem.* **2011**, *123*, 314–317.
[9] a) J. R. Betley, S. Cesaro-Tadic, A. Mekhalfia, J. H. Rickard, H. Denham, L. J. Partridge, A. Pluckthun, G. M. Blackburn, *Angew. Chem. Int. Ed.* **2002**, *41*, 775–777; *Angew. Chem.* **2002**, *114*, 801–803; b) Q. Zhu, X.

Huang, G. Y. J. Chen, S. Q. Yao, *Tetrahedron Lett.* **2003**, *44*, 2669 – 2672; c) K. Shen, L. X. Qi, M. Ravula, K. Klimaszewski, *Bioorg. Med. Chem. Lett.* **2009**, *19*, 3264 – 3267; d) K. A. Kalesh, L. P. Tan, K. Lu, L. Q. Gao, J. G. Wang, S. Q. Yao, *Chem. Commun.* **2010**, *46*, 589 – 591; e) Y. Yuang, C. C. Kuo, C. Y. Chu, Y. H. Huang, Y. L. Hu, J. J. Lin, L. C. Lo, *Tetrahedron* **2010**, *66*, 4521 – 4529; f) N. W. Polaske, B. D. Kelly, J. Ashworth-Sharpe, C. Bieniarz, *Bioconjugate Chem.* **2016**, *27*, 660 – 666.

[10] a) C. S. Tsai, Y. K. Li, L. C. Lo, *Org. Lett.* **2002**, *4*, 3607 – 3610; b) L. M. Chauvigné-Hines, L. N. Anderson, H. M. Weaver, J. N. Brown, P. K. Koech, C. D. Nicora, B. A. Hofstad, R. D. Smith, M. J. Wilkins, S. J. Callister, A. T. Wright, *J. Am. Chem. Soc.* **2012**, *134*, 20521 – 20532; c) M. Ichikawa, Y. Ichikawa, *Bioorg. Med. Chem. Lett.* **2001**, *11*, 1769 – 1773; d) M. Kurogochi, S. I. Nishimura, Y. C. Lee, *J. Biol. Chem.* **2004**, *279*, 44704 – 44712; e) H. Hinou, M. Kurogochi, H. Shimizu, S. I. Nishimura, *Biochemistry* **2005**, *44*, 11669 – 11675; f) C. P. Lu, C. T. Ren, Y. N. Lai, S. H. Wu, W. M. Wang, J. Y. Chen, L. C. Lo, *Angew. Chem. Int. Ed.* **2005**, *44*, 6888 – 6892; *Angew. Chem.* **2005**, *117*, 7048 – 7052; g) Y. T. Chang, C. M. Cheng, Y. Z. Su, W. T. Lee, J. S. Hsu, G. C. Liu, T. L. Cheng, Y. M. Wang, *Bioconjugate Chem.* **2007**, *18*, 1716 – 1727; h) S. H. Chen, Y. T. Kuo, G. Singh, T. L. Cheng, Y. Z. Su, T. P. Wang, Y. Y. Chiu, J. J. Lai, C. C. Chang, T. S. Jaw, S. C. Tzou, G. C. Liu, Y. M. Wang, *Inorg. Chem.* **2012**, *51*, 12426 – 12435; i) T. C. Cheng, S. R. Roffler, S. C. Tzou, K. H. Chuang, Y. C. Su, C. H. Chuang, C. H. Kao, C. S. Chen, I. H. Harn, K. Y. Liu, T. L. Cheng, Y. L. Leu, *J. Am. Chem. Soc.* **2012**, *134*, 3103 – 3110; j) H. Kai, H. Hinou, S. I. Nishimura, *Bioorg. Med. Chem.* **2012**, *20*, 2739 – 2746; k) H. Kai, H. Hinou, K. Naruchi, T. Matsushita, S. I. Nishimura, *Chem. Eur. J.* **2013**, *19*, 1364 – 1372; l) Y. L. Hsu, M. Nandakumar, H. Y. Lai, T. C. Chou, C. Y. Chu, C. H. Lin, L. C. Lo, *J. Org. Chem.* **2015**, *80*, 8458 – 8463.

[11] C. H. Tai, C. P. Lu, S. H. Wu, L. C. Lo, *Chem. Commun.* **2014**, *50*, 6116 – 6119.

[12] a) Q. Shao, Y. Zheng, X. Dong, K. Tang, X. Yan, B. Xing, *Chem. Eur. J.* **2013**, *19*, 10903 – 10910; b) W. Mao, L. Xia, Y. Wang, H. Xie, *Chem. Asian J.* **2016**, *11*, 3493 – 3497.

[13] a) T. Komatsu, K. Kikuchi, H. Takakusa, K. Hanaoka, T. Ueno, M. Kamiya, Y. Urano, T. Nagano, *J. Am. Chem. Soc.* **2006**, *128*, 15946 – 15947; b) R. Zhu, S. Wang, Z. Xue, J. Han, S. Han, *Chem. Commun.* **2018**, *54*, 11566 – 11569.

[14] a) J. E. Coleman, *Annu. Rev. Biophys. Biomol. Struct.* **1992**, *21*, 441 – 483; b) N. K. Tonks, *Nat. Rev. Mol. Cell Biol.* **2006**, *7*, 833 – 846; c) Y. Shi, *Cell* **2009**, *139*, 468 – 484.

[15] a) O. Maldonado, R. Demasi, Y. Maldonado, M. Taylor, F. Troncale, R. Vender, *J. Clin. Gastroenterol.* **1998**, *27*, 342 – 345; b) A. R. Khan, F. R. Awan, S. S. Najam, M. Islam, T. Siddique, M. Zain, *J. Pak. Med. Assoc.* **2015**, *65*, 1182 – 1185; c) J. F. Liu, D. R. Wang, J. Li, Y. Xiong, B. Liu, C. C. Wei, S. M. Wu, J. Lin, M. Liu, *J. Stroke Cerebrovasc.* **2016**, *25*, 2448 – 2452.

[16] a) H. W. Liu, X. X. Hu, L. Zhu, K. Li, Q. Rong, L. Yuan, X. B. Zhang, W. Tan, *Talanta* **2017**, *175*, 421 – 426; b) Y. Tan, L. Zhang, K. H. Man, R. Peltier, G. Chen, H. Zhang, L. Zhou, F. Wang, D. Ho, S. Q. Yao, Y. Hu, H. Sun, *ACS Appl. Mater. Interfaces* **2017**, *9*, 6796 – 6803; c) C. S. Park, T. H. Ha, M. Kim, N. Raja, H. S. Yun, M. J. Sung, O. S. Kwon, H. Yoon, C. S. Lee, *Biosens. Bioelectron.* **2018**, *105*, 151 – 158; d) R. Yan, Y. Hu, F. Liu, S. Wei, D. Fang, A. J. Shuhendler, H. Liu, H. Y. Chen, D. Ye, *J. Am. Chem. Soc.* **2019**, *141*, 10331 – 10341.

[17] J. Zhou, X. Du, C. Berciu, H. He, J. Shi, D. Nicastro, B. Xu, *Chem* **2016**, *1*, 246 – 263.

[18] H. C. Kolb, M. G. Finn, K. B. Sharpless, *Angew. Chem. Int. Ed.* **2001**, *40*, 2004 – 2021; *Angew. Chem.* **2001**, *113*, 2056 – 2075.

[19] C. W. Lin, M. Sasaki, M. L. Orcutt, H. Miyayama, R. M. Singer, *J. Histochem. Cytochem.* **1976**, *24*, 659 – 667.

[20] a) V. Ntziachristos, C. Bremer, R. Weissleder, *Eur. Radiol.* **2003**, *13*, 195 – 208; b) S. A. Hilderbrand, R. Weissleder, *Curr. Opin. Chem. Biol.* **2010**, *14*, 71 – 79; c) Z. Guo, S. Park, J. Yoon, I. Shin, *Chem. Soc. Rev.* **2014**, *43*, 16 – 29.

[21] H. J. Chen, C. Y. Chew, E. H. Chang, Y. W. Tu, L. Y. Wei, B. H. Wu, C. H. Chen, Y. T. Yang, S. C. Huang, J. K. Chen, I. C. Chen, K. T. Tan, *J. Am. Chem. Soc.* **2018**, *140*, 5224 – 5234.

Manuscript received: July 29, 2019
Revised manuscript received: August 30, 2019
Accepted manuscript online: September 10, 2019
Version of record online: ■■ ■■, 0000

FULL PAPER

Fluorescent Probes

*H. Song, Y. Li, Y. Chen, C. Xue, H. Xie**

■■ – ■■

Highly Efficient Multiple-Labeling Probes for the Visualization of Enzyme Activities

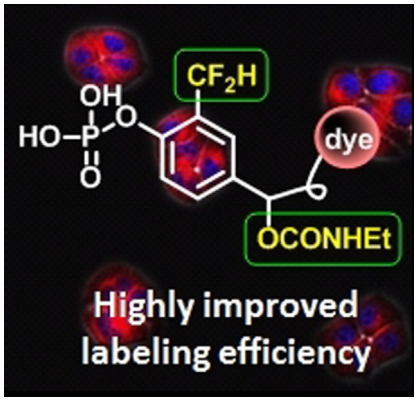

Visualizing the activity: An investigation on the labeling efficiency and structure of quinone methide (QM) based trapping unit is presented, from which a QM with multiple leaving groups was identified as an optimal trapping unit. An alkaline phosphatase (ALP) immobilizing reagent featured with this multiple-labeling trapping unit exhibited upon enzymatic activation a lower nonspecific binding and, remarkably, a significantly higher labeling efficiency over other immobilizing reagents. In vitro and in vivo visualization of the ALP activity is also reported.